

## Defects composed of kinks and $Q$ -balls: Analytical solutions and stability

A. Alonso-Izquierdo<sup>1,2</sup> and C. Garzón Sánchez<sup>1</sup>

<sup>1</sup>*Departamento de Matematica Aplicada, University of Salamanca,  
Casas del Parque 2, 37008 Salamanca, Spain*

<sup>2</sup>*IUFFyM, University of Salamanca, Plaza de la Merced 1, 37008 Salamanca, Spain*



(Received 11 March 2023; accepted 19 May 2023; published 6 June 2023)

In this paper all the defect-type solutions in a family of scalar field theories with a real and a complex field in  $(1 + 1)$ -dimensional Minkowski spacetime have been analytically identified. Three types of solutions have been found: (a) topological kinks without the presence of  $Q$ -balls, (b) defects that consist of a topological kink coupled with a  $Q$ -ball, and (c) a one-parameter family of solutions where a  $Q$ -ball is combined with a nontopological soliton. The properties of these solutions and its linear stability are also discussed.

DOI: [10.1103/PhysRevD.107.125004](https://doi.org/10.1103/PhysRevD.107.125004)

### I. INTRODUCTION

$Q$ -balls are time-dependent nontopological solitons arising in nonlinear field theories that, in addition, conserve a Noether charge associated with a global  $U(1)$  symmetry [1,2]. One of the most relevant roles of  $Q$ -balls in physics involves the explanation of baryogenesis in cosmology. In some supersymmetric extensions of the standard model it was shown that  $Q$ -balls can be produced in the early Universe in such a way that the production mechanism of the baryon asymmetry and the presence of dark matter can be explained at once, see [3]. In these theories, the lightest supersymmetric particles are ideal candidates for dark matter. The nature of these particles depends on the specific model and the supersymmetry breaking process that are considered in the cosmological evolution. For this reason, Higgsino-, bino-, or winolike neutralinos have been proposed as dominant components of the dark matter in different scenarios. The Affleck-Dine (AD) mechanism, which can be used to explain baryogenesis, is based on the dynamics of a complex scalar field  $\phi$  (called the AD field). This field carries a conserved charge, which can be interpreted as the baryon number. During inflation, the expectation value of the AD field takes very large values but, after the end of inflation, this field starts a coherent oscillation. Then, the AD field gets a internal rotation frequency, which leads to a baryon number generation. The coherent oscillation of the AD field is generally unstable and fragments into small  $Q$ -balls [4]. However, in some

models these solutions have a long lifetime and its decay temperature is likely to be well below the freeze-out temperature of the lightest supersymmetric particles. This leads to the nonthermal production of the dark matter. The number density of these particles depends on the lifetime of the  $Q$ -ball. It has been found that to explain the experimental abundance of baryons and dark matter in the Universe, it is needed that  $Q$ -balls have a very long lifetime [5–9].

On the other hand, the existence of  $Q$ -balls has been proposed in high temperature superconductors in the “nested Hubbard model” by Mukhin [10]. In some materials, when temperature is higher than a critical temperature  $T_c$ , superconductivity emerges related with the presence of a pseudogap (where, within the band-theory approximation, some regions of the Fermi surface become gapped, while other parts retain their conducting properties, and when doping is increased, the gapped portion diminishes and the materials become more metallic). In this situation, Cooper pairs are formed because couples of fermions form a bound state by exchanging fluctuations of charge/spin density waves (CDWs/SDWs). In these conditions,  $Q$ -balls can arise as a condensate of these elementary bosonic excitations. Because all the Fourier components of the CDWs/SDWs have a  $U(1)$  symmetry, the conserved Noether charge  $Q$  carried by these nontopological solitons corresponds with the total number of these excitations. In this case, the internal rotation frequency is identified with the frequency of the fundamental Fourier component of the CDWs/SDWs, which is called the “bosonic Matsubara frequency,” see [10–13].

Another scenario in condensed matter where  $Q$ -balls arise is given by some magnetic materials at low temperature. When a magnetic field is applied to these materials, spins tend to align toward the magnetic field direction.

*Published by the American Physical Society under the terms of the Creative Commons Attribution 4.0 International license. Further distribution of this work must maintain attribution to the author(s) and the published article's title, journal citation, and DOI. Funded by SCOAP<sup>3</sup>.*

However, small precession movements emerge in these spins. These spin excitations behave as quasiparticles, which are referred to as magnons. At this stage, the material manifests a phase coherence giving place to a superconductor with homogeneous precession density. At low temperature, this configuration develops instabilities (called ‘‘Suhl instabilities’’) and pairs of spin waves are formed at some points, which travel along the substrate. These are named ‘‘persistent signals’’ and can be interpreted as a condensate of magnons. These persistent signals can be described as  $Q$ -balls, where the Noether charge  $Q$  is the total number of magnons, and the internal rotation frequency is identified with the precession frequency, see [14,15].

In the pioneering paper [16], Friedberg *et al.* investigated the presence of this class of solutions in a theoretical model involving a complex scalar field coupled to a real scalar field in three space dimensions. The nonlinear couplings between the fields arising in this model are characterized by a quartic polynomial, which means that the theory is renormalizable. The authors describe the  $Q$ -balls present in the model and provide a thorough scheme to analyze the linear stability of these solutions when small fluctuations that maintain the conserved Noether charge constant are applied. Theorem 3 in that paper establishes that the necessary and sufficient conditions to guarantee the classical stability of  $Q$ -balls are that the small fluctuation operator evaluated on these solutions has only one negative eigenvalue and that the derivative of the Noether charge  $Q$  with respect to the internal rotation frequency  $\omega$  is negative. In this prescription, the frequency  $\omega$  is chosen as positive. A similar theorem was proven for the first time by Vakhitov [17] and Kolokolov [18] in a different framework. The authors found the same stability criterion for the principal mode of nonlinear wave equations in a medium with nonlinearity saturation. The existence of  $Q$ -balls and their properties have been studied in different contexts, see [19] and references therein. Some of these particular scenarios involve complex scalar field theories [20–24], Abelian gauge theories [25–28], Chern-Simons theories [29–31], non-Abelian theories [32–34], etc.

In general, models involving  $Q$ -balls are so complicated that it is not possible to obtain analytical expressions for these nontopological solitons. In recent works [35–37],  $Q$ -balls have been exactly calculated for some theories with one complex scalar field in  $(1+1)$  dimensions. In this paper, we address the study of a one-parameter family of field theories in  $(1+1)$  dimensions, which involves the coupling between a real and a complex field. The model parameter can be understood as a measure of the deformation of the model with respect to an  $O(3)$  invariant linear sigma model. Remarkably, all the defect-type solutions can be analytically identified, which makes it easier to study their properties. There exist three different types of these solutions. First, a standard topological kink living in the

real field component emerges without the presence of  $Q$ -balls. The second class can be described as defects consisting of one topological kink defined in the real component and one  $Q$ -ball spinning along the complex field axis. From our point of view, this is a new type of solution endowed with novel properties. For example, this coupling between a topological kink and a  $Q$ -ball determines a new scenario that seems to elude the applicability of the previously mentioned Theorem 3. These solutions do not verify any of the hypotheses introduced in Theorem 3. Despite this fact, they are stable, as it will be proved in this paper. Finally, a one-parametric family of defects involving the presence of a nontopological soliton together with a  $Q$ -ball is also identified. In this case, Theorem 3 can be applied to demonstrate that these solutions are unstable.

The organization of this paper is as follows: the family of deformed  $O(3)$  linear sigma models addressed in this work and its properties are introduced in Sec. II. The previously mentioned defects composed of kinks and  $Q$ -balls are analytically identified and described in Sec. III. Section IV is dedicated to investigate the linear stability of these composite solitons. Finally, the conclusions of this work are summarized in Sec. V.

## II. THE MODEL

We shall deal with a field theory immersed in a  $(1+1)$ -dimensional Minkowski spacetime, which involves the coupling between one real and one complex scalar field. The dynamics of this model is characterized by the action functional

$$S = \int d^2x \left[ \frac{1}{2} \partial_\mu \phi \partial^\mu \phi + \frac{1}{2} \partial_\mu \bar{\psi} \partial^\mu \psi - U(\phi, |\psi|) \right], \quad (1)$$

where  $\phi$  and  $\psi = \psi_1 + i\psi_2$  are, respectively, the real and the complex scalar fields, that is,  $\phi \in \text{Maps}(\mathbb{R}^{1,1}, \mathbb{R})$  and  $\psi \in \text{Maps}(\mathbb{R}^{1,1}, \mathbb{C})$ . In (1),  $\bar{\psi}$  stands for the complex conjugate of  $\psi$ . As usual in this context, the Minkowski metric  $g_{\mu\nu}$  is chosen as  $g_{00} = -g_{11} = 1$  and  $g_{12} = g_{21} = 0$ . The potential term  $U(\phi, |\psi|)$  which will be investigated in this paper is given by the positive semidefinite expression

$$U(\phi, |\psi|; \sigma) = \frac{1}{2} \left( \phi^2 + |\psi|^2 - 1 \right)^2 + \frac{1}{2} \sigma^2 |\psi|^2, \quad (2)$$

with  $\sigma \in \mathbb{R}$ . The relation (2) is a quartic polynomial in the real field  $\phi$  and the modulus of the complex field  $\psi$ . Note that, for  $\sigma = 0$ ,

$$U(\phi, |\psi|; 0) = \frac{1}{2} \left( \phi^2 + \psi_1^2 + \psi_2^2 - 1 \right)^2, \quad (3)$$

and, therefore, this system can be understood as a deformation of an  $O(3)$  linear sigma model, where the parameter  $\sigma$  measures the asymmetry with respect to the rotationally

invariant situation. The potential has two critical points at  $(\phi, \psi) = v_{\pm} = (\pm 1, 0)$ , where the potential vanishes,  $U(v_{\pm}) = 0$ . The Hessian matrix of (2) evaluated at these points is

$$\mathcal{H}[v_{\pm}] = \left( \begin{array}{cc} \frac{\partial^2 U}{\partial \phi^2} & \frac{\partial^2 U}{\partial \phi \partial |\psi|} \\ \frac{\partial^2 U}{\partial \phi \partial |\psi|} & \frac{\partial^2 U}{\partial |\psi|^2} \end{array} \right) \Bigg|_{v_{\pm}} = \begin{pmatrix} 4 & 0 \\ 0 & \sigma^2 \end{pmatrix},$$

which means that  $v_{\pm}$  are minima of the potential, as expected. Despite the fact that the  $O(3)$  symmetry associated with (3) is broken for  $\sigma \neq 0$ , a  $U(1)$  symmetry remains. Clearly, the model is invariant with respect to the global transformation  $\psi \rightarrow e^{i\beta} \psi$ , which leads to the conserved Noether charge

$$Q = \frac{1}{2i} \int (\bar{\psi} \partial_t \psi - \psi \partial_t \bar{\psi}) dx. \quad (4)$$

The field equations obtained from the action functional (1) read

$$\begin{aligned} \frac{\partial^2 \phi}{\partial t^2} - \frac{\partial^2 \phi}{\partial x^2} + \frac{\partial U(\phi, |\psi|)}{\partial \phi} &= 0, \\ \frac{\partial^2 \psi}{\partial t^2} - \frac{\partial^2 \psi}{\partial x^2} + \frac{\psi}{|\psi|} \frac{\partial U(\phi, |\psi|)}{\partial |\psi|} &= 0. \end{aligned} \quad (5)$$

In this paper, we are interested in searching for solutions that comprise a kink (defined by the real field) and a  $Q$ -ball (defined by the complex field). For this reason, the ansatz

$$\phi(x, t) = f(x), \quad \psi(x, t) = g(x) e^{i\omega t} \quad (6)$$

is substituted into the field equations (5). This leads to the system of ordinary differential equations

$$\frac{\partial^2 f}{\partial x^2} = \frac{\partial U(f, g)}{\partial f}, \quad \frac{\partial^2 g}{\partial x^2} = \frac{\partial U(f, g)}{\partial g} - \omega^2 g \quad (7)$$

for the real functions  $f(x)$  and  $g(x)$ . The quantity  $\omega$  in (6) is the internal rotation frequency of the  $Q$ -ball. Without loss of generality, we can consider that  $\omega$  is positive. The potential term  $U$  in (7) becomes now

$$U(f, g; \sigma) = \frac{1}{2} (f^2 + g^2 - 1)^2 + \frac{1}{2} \sigma^2 g^2, \quad (8)$$

while the conserved Noether charge (4) is

$$Q = \omega \int_{-\infty}^{\infty} (g(x))^2 dx. \quad (9)$$

The energy functional  $E[f, g]$  is written in this case as the integral over the space coordinate of the energy density  $\mathcal{E}[f, g]$ , i.e.,

$$\begin{aligned} E[f, g] &= \int_{-\infty}^{\infty} \mathcal{E}[f, g] dx \\ &= \int_{-\infty}^{\infty} dx \left[ \frac{1}{2} \left( \frac{\partial f}{\partial x} \right)^2 + \frac{1}{2} \left( \frac{\partial g}{\partial x} \right)^2 \right. \\ &\quad \left. + \frac{1}{2} \omega^2 g^2 + U(f, g; \sigma) \right], \end{aligned} \quad (10)$$

which implies that the solutions of the system must satisfy the following asymptotic conditions:

$$\begin{aligned} \lim_{x \rightarrow \pm\infty} f(x) &\in \mathcal{M}, \quad \lim_{x \rightarrow \pm\infty} \frac{df}{dx} = 0, \\ \lim_{x \rightarrow \pm\infty} g(x) &= \lim_{x \rightarrow \pm\infty} \frac{dg}{dx} = 0, \end{aligned} \quad (11)$$

in order to keep the total energy (10) finite. In (11),  $\mathcal{M} = \{-1, 1\}$ , the set of possible values of the real field leading to zeros of the potential term  $U(f, g)$ . It is also clear from (7) that the problem involves the effective potential

$$\begin{aligned} \bar{U}(f, g; \sigma) &= U(f, g; \sigma) - \frac{1}{2} \omega^2 g^2 \\ &= \frac{1}{2} (f^2 + g^2 - 1)^2 + \frac{1}{2} (\sigma^2 - \omega^2) g^2 \\ &= U(f, g; \Omega), \end{aligned} \quad (12)$$

which has the same functional form as (8), but with a new model parameter  $\Omega$  defined as

$$\Omega^2 = \sigma^2 - \omega^2. \quad (13)$$

Now, Eqs. (7) can be written in the more compact form

$$\frac{\partial^2 f}{\partial x^2} = \frac{\partial \bar{U}(f, g)}{\partial f}, \quad \frac{\partial^2 g}{\partial x^2} = \frac{\partial \bar{U}(f, g)}{\partial g}. \quad (14)$$

The effective potential (12) depends on the internal rotation frequency. In Fig. 1, the potential  $\bar{U}(f, g; \sigma)$  has been depicted for several values of  $\omega$  with a fixed value of the model parameter  $\sigma$ . The Hessian matrix of this effective potential evaluated on the points  $v_{\pm}$  reads

$$\bar{\mathcal{H}}[v_{\pm}] = \left( \begin{array}{cc} \frac{\partial^2 \bar{U}}{\partial \phi^2} & \frac{\partial^2 \bar{U}}{\partial \phi \partial |\psi|} \\ \frac{\partial^2 \bar{U}}{\partial \phi \partial |\psi|} & \frac{\partial^2 \bar{U}}{\partial |\psi|^2} \end{array} \right) \Bigg|_{v_{\pm}} = \begin{pmatrix} 4 & 0 \\ 0 & \sigma^2 - \omega^2 \end{pmatrix}.$$

This means that  $v_{\pm}$  are absolute minima of  $\bar{U}(f, g)$  for  $\omega^2 < \sigma^2$ , but they become saddle points in the other case. For this reason, a necessary condition for the existence of the topological defects (which we are interested in) is

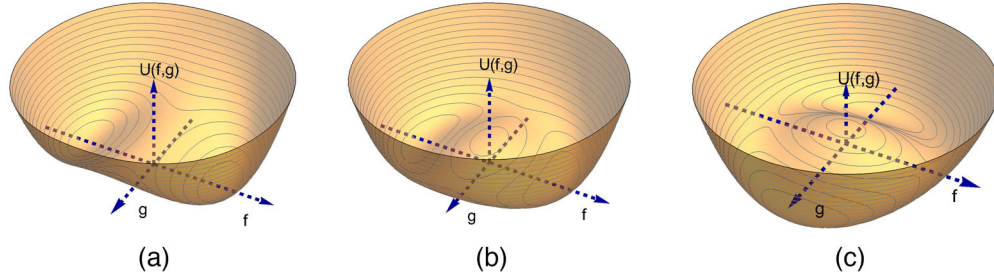


FIG. 1. Graphics of the effective potential  $\bar{U}(f, g; \sigma)$  for the model parameter  $\sigma = 1.5$  and several values of the internal rotation frequency: (a)  $\omega = 0$ , (b)  $\omega = 1.2$ , and (c)  $\omega = 1.8$ .

$$\omega^2 < \sigma^2.$$

$$\frac{\partial^2 f}{\partial x^2} = 2f(f^2 + g^2 - 1), \quad \frac{\partial^2 g}{\partial x^2} = 2g(f^2 + g^2 - 1) + \Omega^2 g. \quad (18)$$

Solving the system (14) together with the conditions (11) is tantamount to finding solutions asymptotically beginning and ending at the vacuum points  $v_{\pm}$  for Newton equations in which  $x$  plays the role of time, the particle position is determined by  $(f, g)$ , and the potential energy of the particle is  $V(f, g) = -U(f, g)$ . Note that the differential equations (14), or equivalently (7), can be derived from the effective functional

$$\bar{E}[f, g; \sigma] = \int dx \left[ \frac{1}{2} \left( \frac{df}{dx} \right)^2 + \frac{1}{2} \left( \frac{dg}{dx} \right)^2 + \bar{U}(f, g; \sigma) \right], \quad (15)$$

keeping  $\omega$  fixed, i.e.,  $\delta \bar{E}[f, g; \sigma]|_{\omega} = 0$ . Note that the following relation between the functionals (10) and (15)

$$E[f, g; \sigma] = \bar{E}[f, g; \sigma] + \omega Q \quad (16)$$

holds. Alternatively, Eqs. (7) can be derived as a stationary point of the functional (10), keeping  $Q$  fixed, i.e.,  $(\delta E)|_Q = 0$ . All of this means that  $\bar{E}[f, g; \sigma]$  is a Legendre transformation derived from the functional (10), see [16], which leads to the relations

$$\frac{d\bar{E}}{d\omega} = -Q \quad \text{and} \quad \frac{dE(Q)}{dQ} = \omega. \quad (17)$$

### III. FAMILIES OF DEFECTS COMPOSED OF KINKS AND $Q$ -BALLS

In this section, we shall analytically identify the previously mentioned defects involving the coexistence of a kink and a  $Q$ -ball. Equations (7) [or, equivalently, (14)] are written for our model as

These equations have been well studied in the context of multicomponent kink solutions arising in the Montonen-Sarker-Trullinger-Bishop model. A thorough summary of the history and the analytical properties of this model can be found in [38] and references therein. The key point is that Eqs. (18) can be solved by introducing elliptic variables in the internal space  $(f, g)$  whose isocoordinate curves consist of ellipses and hyperbolas with foci  $F_{\pm} = (\pm\Omega, 0)$ . In these variables the differential equations (18) are separable. It can be checked that for  $\Omega^2 = \sigma^2 - \omega^2 \geq 1$  only a topological kink and its antikink arise and there is no room for  $Q$ -balls in the system. These topological defects can be expressed as

$$\mathcal{K}_1(x) = ((-1)^{\alpha} \tanh \bar{x}, 0), \quad \alpha = 0, 1, \quad (19)$$

which carry a total energy  $E[\mathcal{K}_1(x)] = 4/3$ . In (19),  $\bar{x} = x - x_0$ , where  $x_0$  can be interpreted as the center of the solution. Note that the multicomponent notation  $(f, e^{i\omega t} g)$  has been employed in (19) to write the solutions. Therefore, if the second component is zero, the solution does not involve  $Q$ -balls. Note that

$$Q[\mathcal{K}_1(x)] = 0. \quad (20)$$

On the other hand, for the regime  $0 < \Omega^2 < 1$ , the presence of  $Q$  balls is possible. This implies that the necessary and sufficient condition for the existence of defects consisting of kinks and  $Q$ -balls in the model (2) is

$$\max\{0, \sigma^2 - 1\} < \omega^2 < \sigma^2. \quad (21)$$

The previously described solutions are simply given by the expression

$$\mathcal{K}_2(x, t) = \left( (-1)^{\alpha} \tanh(\Omega \bar{x}), e^{i\omega t} \sqrt{1 - \Omega^2} \operatorname{sech}(\Omega \bar{x}) \right), \quad \alpha = 0, 1, \quad (22)$$

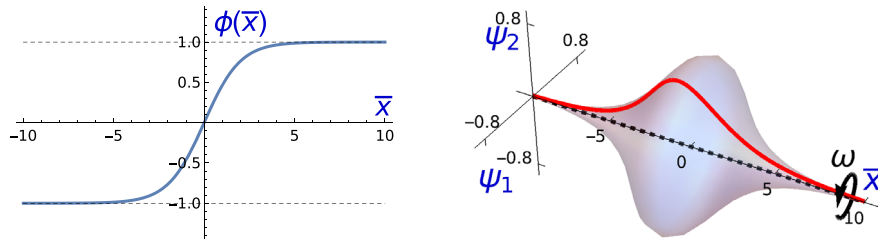


FIG. 2. Graphics of the solution  $\mathcal{K}_2(x, t)$  composed by a topological kink in the real component and a  $Q$ -ball in the complex component of the internal space for the particular value  $\Omega = 0.5$  and  $\alpha = 0$ .

which has been illustrated in Fig. 2. It can be observed that the solution consists of a kink profile in the real field axis and a nontopological soliton ( $Q$ -ball) spinning in the complex component of the internal space with rotational frequency  $\omega$ .<sup>1</sup>

For the sake of completeness, the Noether charge (9) for this type of defect is

$$Q[\mathcal{K}_2(x, t)] = \frac{2\omega(1 - \Omega^2)}{\Omega} = 2\omega \frac{1 - \sigma^2 + \omega^2}{\sqrt{\sigma^2 - \omega^2}}, \quad (23)$$

while its total energy follows the form

$$E[\mathcal{K}_2(x, t)] = \frac{2(2\omega^4 - \sigma^4 - \sigma^2(\omega^2 - 3))}{3\sqrt{\sigma^2 - \omega^2}}. \quad (24)$$

The previous expressions are restricted to the range  $\omega^2 \in (\sigma^2 - 1, \sigma^2)$  where the solutions (22) are well defined. Note that  $\frac{dQ[\mathcal{K}_2(x, t)]}{d\omega} = \Omega^{-3}[2\sigma^2(1 - \Omega^2) + 4\omega^2\Omega^2] > 0$ . In the usual models found in the literature, this condition implies that the  $Q$ -balls are unstable, as stated by Theorem 3 in [16]. However, as it will be proved in the next section, the solutions (22) elude the hypotheses of this theorem and, indeed, they are stable against small fluctuations that preserve the Noether charge (23). It seems that the topological nature of the kink living in the real component protects the  $Q$ -ball constituent from decaying into the vacuum configuration. From our point of view, this behavior turns the composite defects (22) into a new type of solution in this context.

In addition to solutions (19) and (22), there exists a one-parametric family of solutions, which turn out to be a combination of a nontopological kink and a  $Q$ -ball. It can be checked that the expression

$$\mathcal{K}_3(x, t; \gamma) = \left( (-1)^\alpha \frac{\Omega_- \cosh(\Omega_+ x_+) - \Omega_+ \cosh(\Omega_- x_-)}{\Omega_- \cosh(\Omega_+ x_+) + \Omega_+ \cosh(\Omega_- x_-)}, \frac{2\Omega_+ \Omega_- e^{i\omega t} \sinh \bar{x}}{\Omega_- \cosh(\Omega_+ x_+) + \Omega_+ \cosh(\Omega_- x_-)} \right) \quad (25)$$

with  $\Omega_\pm = 1 \pm \Omega$ ,  $x_\pm = \bar{x} - \gamma\Omega(\Omega \mp 1)$  and  $\alpha = 0, 1$  satisfies the field equations (5). Every member of the  $\mathcal{K}_3(x, t; \gamma)$  family is determined by the value of the parameter  $\gamma \in \mathbb{R}$ . All of them are characterized by the presence of a nontopological kink in the real component (asymptotically beginning and ending at the same vacuum) and the appearance of a node in the  $Q$ -ball profile located at  $\bar{x} = 0$ . In Fig. 3, the defect  $\mathcal{K}_3(x, t; 0)$  is depicted. For this case with  $\gamma = 0$  the profiles of the solution are symmetric with respect to the spatial point  $\bar{x} = 0$ . If the two partial Noether charges

$$Q_1 = \omega \int_{-\infty}^0 (g(\bar{x}))^2 d\bar{x}, \quad Q_2 = \omega \int_0^{\infty} (g(\bar{x}))^2 d\bar{x}$$

are defined (such that  $Q = Q_1 + Q_2$ ), it is clear that for the  $\mathcal{K}_3(x, t; 0)$  solution the relation  $Q_1 = Q_2 = Q/2$  holds. In

Fig. 4, the member of the  $\mathcal{K}_3(x, t; \gamma)$  family with  $\gamma = 3$  is plotted. Now, the solution is asymmetric and the partial charges  $Q_i$  are different. In this particular case, the partial charge  $Q_1$  is greater than  $Q_2$ . This behavior continues as the value of the family parameter  $\gamma$  increases. Indeed, when  $\gamma$  is very large, the value of  $Q_2$  tends to zero and  $Q_1$  tends to the Noether charge of the  $\mathcal{K}_2(x, t)$  solution. This means that the  $\mathcal{K}_3(x, t; \gamma)$  defects can be understood as a nonlinear combination of a  $\mathcal{K}_2(x, t)$  and a  $\mathcal{K}_1(x, t)$  solution.

Another remarkable property of the previously mentioned solutions is expressed as sum rules connecting the total energies and the Noether charges of the defects. All the members of the  $\mathcal{K}_3(x, \gamma)$  family have the same Noether charge  $Q$  and the same total energy  $E$ . In addition to this, its conserved charge  $Q$  amounts to that of the  $\mathcal{K}_2(x)$  solution, while its energy is equal to the sum of the energies of the  $\mathcal{K}_1(x)$  and  $\mathcal{K}_2(x)$  solutions,

$$Q[\mathcal{K}_3(x, t; \gamma)] = Q[\mathcal{K}_2(x, t)], \quad (26)$$

<sup>1</sup>The solution (22) for the special case  $\sigma = 0$  was described by Montonen in [39].

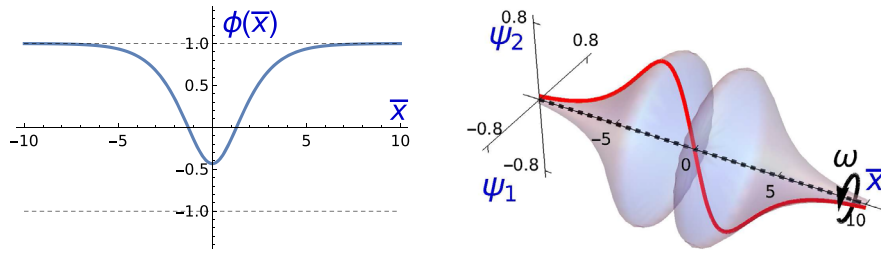


FIG. 3. Graphics of the solution  $\mathcal{K}_3(x, t; \gamma)$  composed of a nontopological soliton in the real component and a  $Q$ -ball in the complex component of the internal space for the particular values  $\sigma = 0.5$ ,  $\omega = 0.25$ ,  $\alpha = 0$ , and  $\gamma = 0$ .

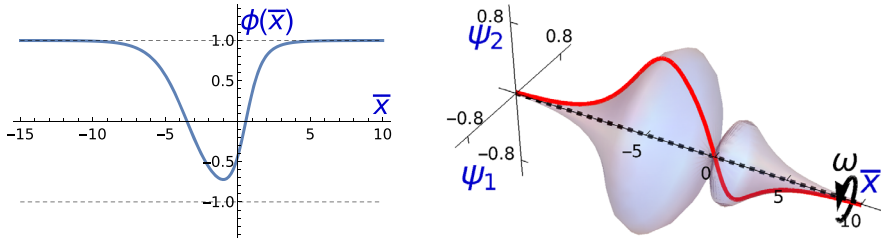


FIG. 4. Graphics of the solution  $\mathcal{K}_3(x, t; \gamma)$  composed of a nontopological soliton in the real component and a  $Q$ -ball in the complex component of the internal space for the particular values  $\sigma = 0.5$ ,  $\omega = 0.25$ ,  $\alpha = 0$ , and  $\gamma = 3$ .

$$E[\mathcal{K}_3(x, t; \gamma)] = E[\mathcal{K}_1(x, t)] + E[\mathcal{K}_2(x, t)]. \quad (27)$$

These results can be analytically proved from the Legendre transformations introduced in Sec. II. From (17), it is clear that

$$\begin{aligned} Q[\mathcal{K}_3(x, \gamma)] &= -\frac{d\bar{E}[\mathcal{K}_3(x, \gamma)]}{d\omega} = -\frac{d\bar{E}[\mathcal{K}_1(x)]}{d\omega} - \frac{d\bar{E}[\mathcal{K}_2(x)]}{d\omega} \\ &= Q[\mathcal{K}_1(x)] + Q[\mathcal{K}_2(x)] = Q[\mathcal{K}_2(x)], \end{aligned}$$

which justifies (26). Here, we have used that  $\bar{E}[\mathcal{K}_3(x, \gamma)] = \bar{E}[\mathcal{K}_1(x)] + \bar{E}[\mathcal{K}_2(x)]$ , which can be manifestly demonstrated by exploiting the separability of the functional  $\bar{E}(f, g)$  in elliptic coordinates, see [38]. From (16) and (26), the relation (27) is directly obtained. The identities (26) and (27) corroborate the previously mentioned interpretation of the  $\mathcal{K}_3(x, t; \gamma)$  solutions and lead to the following results:

$$\begin{aligned} Q[\mathcal{K}_3(x, \gamma)] &= 2\omega \frac{1 - \sigma^2 + \omega^2}{\sqrt{\sigma^2 - \omega^2}} \quad \text{and} \\ E[\mathcal{K}_3(x, \gamma)] &= \frac{4}{3} + \frac{2(2\omega^4 - \sigma^4 - \sigma^2(\omega^2 - 3))}{3\sqrt{\sigma^2 - \omega^2}}. \end{aligned}$$

### A. Stability analysis of the $Q$ -balls

In this section, the (classical) linear stability of the solutions described in Sec. II is investigated following the prescription established in the seminal paper [16].

In this scheme, a static solution  $\mathcal{K}(x) = (f(x), g(x))$  is perturbed by applying a small fluctuation  $(\delta f, \delta g)$ , which conserves the Noether charge  $Q$ . In order to attain this condition, the internal rotation frequency of the perturbed solution must be varied by the magnitude

$$\delta\omega = -\frac{2\omega^2}{Q} \int_{-\infty}^{\infty} g\delta g dx.$$

Now, the effect of these fluctuations on the energy functional (10) is analyzed. If the total energy  $E[\mathcal{K}(x) + (\delta f, \delta g)]$  of the perturbed configuration is less than  $E[\mathcal{K}(x)]$ , then the solution  $\mathcal{K}(x)$  will be unstable. It can be checked that the variation of the energy functional  $E$  at second order is given by

$$\delta E^{(2)}|_Q = \int_{-\infty}^{\infty} dx \frac{1}{2} (\delta F)^t \mathcal{H}[\mathcal{K}(x)] \delta F + \frac{2\omega^3}{Q} \left( \int_{-\infty}^{\infty} g\delta g dx \right)^2, \quad (28)$$

where the compact notation  $\delta F = (\delta f, \delta g)^t$  has been used. The second-order small fluctuation operator  $\mathcal{H}[\mathcal{K}(x)]$  arising in the previous expression reads

$$\mathcal{H}[\mathcal{K}(x)] = \begin{pmatrix} -\frac{d^2}{dx^2} + \frac{\partial^2 U}{\partial f^2} \Big|_{\mathcal{K}(x)} & \frac{\partial^2 U}{\partial f \partial g} \Big|_{\mathcal{K}(x)} \\ \frac{\partial^2 U}{\partial f \partial g} \Big|_{\mathcal{K}(x)} & -\frac{d^2}{dx^2} + \frac{\partial^2 U}{\partial g^2} \Big|_{\mathcal{K}(x)} - \omega^2 \end{pmatrix}. \quad (29)$$

In particular, for our model where the field potential term  $U(f, g)$  is determined by the expression (8), the operator (29) can be written as

$$\mathcal{H}[\mathcal{K}(x)] = \left( \begin{array}{cc} -\frac{d^2}{dx^2} + 2(3f^2 + g^2 - 1) & 4fg \\ 4fg & -\frac{d^2}{dx^2} + 2(f^2 + 3g^2 - 1) + \Omega^2 \end{array} \right) \Big|_{\mathcal{K}(x)}. \quad (30)$$

### 1. Linear stability analysis for the $\mathcal{K}_2(x)$ solutions

To study the linear stability of the defects  $\mathcal{K}_2(x)$ , composed by a topological kink and a  $Q$ -ball, the expression (22) is substituted into the operator (30). This leads to the particular Schrödinger-type matrix operator

$$\mathcal{H}[\mathcal{K}_2(x)] = \left( \begin{array}{cc} -\frac{d^2}{dx^2} + 4 - 2(2 + \Omega^2)\text{sech}^2(\Omega x) & 4\sqrt{1 - \Omega^2}\text{sech}(\Omega x) \tanh(\Omega x) \\ 4\sqrt{1 - \Omega^2}\text{sech}(\Omega x) \tanh(\Omega x) & -\frac{d^2}{dx^2} + \Omega^2 + 2(2 - 3\Omega^2)\text{sech}^2(\Omega x) \end{array} \right), \quad (31)$$

which depends on the parameter  $\Omega$ . It can be analytically proved that  $\frac{d\mathcal{K}_2(x)}{dx}$  is a zero mode of the operator (31). However, the rest of the eigenvalues of  $\mathcal{H}[\mathcal{K}_2(x)]$  must be numerically calculated. In Fig. 5 the spectrum of this operator is displayed as a function of the parameter  $\Omega$ . The presence of the previously mentioned zero mode with eigenvalue  $\lambda_0 = 0$  can be observed. The continuous spectra emerge on the threshold values  $\Omega^2$  and 4. Note that a discrete eigenfunction with eigenvalue  $\lambda_1$  emerges for  $\Omega > 0.6$  approximately. The crucial point here is that there are no negative eigenvalues. Therefore, the two contributions in (28) are positive, which means that no linear fluctuations can decrease the energy of the solution  $\mathcal{K}_2(x)$ . We have proved that this defect is stable. We recall that Theorem 3 in [16] states that the necessary and sufficient conditions for  $\delta E^{(2)}|_Q > 0$  are (i)  $\mathcal{H}[\mathcal{K}(x)]$  has only one negative eigenvalue and (ii)  $\frac{dQ[\mathcal{K}(x)]}{d\omega} < 0$ . However, in our case there are no negative eigenvalues of the operator  $\mathcal{H}[\mathcal{K}_2(x)]$  and  $\frac{dQ[\mathcal{K}_2(x)]}{d\omega} > 0$ . As a consequence, the  $\mathcal{K}_2(x)$  solutions in our model constitute a counterexample of the universality of the previously mentioned theorem. From our point of view, the assumption that all  $Q$ -ball-type solutions have at least one negative eigenvalue

associated with the second-order small fluctuation operator  $\mathcal{H}$  undermines the generality of the aforementioned theorem. This is clearly valid for models with only one scalar field, where such solutions are nontopological solitons, implying that they must begin and arrive at the vacuum located at the origin of the internal space. In (1 + 1) dimensions, this involves the fact that the solution has a maximum point that characterizes the returning point. Recall that the derivative of the solution with respect to the spatial coordinate is a zero mode, which as mentioned before must have a node. This, in turn, implies that the ground state of the operator  $\mathcal{H}$  must have a negative eigenvalue. However, this does not work in the more general cases, for example, in theories involving a complex scalar field and a real one, since the latter can have a solution that connects two distinct vacuum points, opening the possibility that its small fluctuation operator lacks negative eigenvalues.

### 2. Linear stability analysis for the $\mathcal{K}_3(x; \gamma)$ solutions

The situation is more complicated for the  $\mathcal{K}_3(x; \gamma)$  solutions. Now, the components of the fluctuation operator (30) are

$$\begin{aligned} \mathcal{H}_{11}[\mathcal{K}_3(x; \gamma)] &= -\frac{d^2}{dx^2} - 2 + \frac{6(-\Omega_+ \cosh(\Omega_- x_-) + \Omega_- \cosh(\Omega_+ x_+))^2 + 8\Omega_-^2 \Omega_+^2 \sinh^2 x}{(\Omega_+ \cosh(\Omega_- x_-) + \Omega_- \cosh(\Omega_+ x_+))^2}, \\ \mathcal{H}_{12}[\mathcal{K}_3(x; \gamma)] &= \frac{8\Omega_+ \Omega_- (\Omega_- \cosh(\Omega_+ x_+) - \Omega_+ \cosh(\Omega_- x_-)) \sinh x}{(\Omega_+ \cosh(\Omega_- x_-) + \Omega_- \cosh(\Omega_+ x_+))^2}, \\ \mathcal{H}_{22}[\mathcal{K}_3(x; \gamma)] &= -\frac{d^2}{dx^2} - 2 + \Omega^2 + \frac{2(-\Omega_+ \cosh(\Omega_- x_-) + \Omega_- \cosh(\Omega_+ x_+))^2 + 24\Omega_-^2 \Omega_+^2 \sinh^2 x}{(\Omega_+ \cosh(\Omega_- x_-) + \Omega_- \cosh(\Omega_+ x_+))^2}. \end{aligned}$$

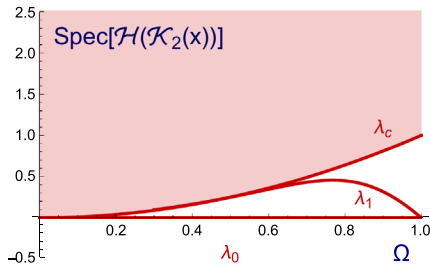


FIG. 5. Spectrum of the second-order small fluctuation operator  $\mathcal{H}[\mathcal{K}_2(x)]$  as a function of the parameter  $\Omega$ .

Despite the intricate form of this operator, some results can be formulated. For example, it can be checked that the expressions  $\frac{\partial \mathcal{K}_3(x;\gamma)}{\partial x}$  and  $\frac{\partial \mathcal{K}_3(x;\gamma)}{\partial \gamma}$  are zero modes of the operator  $\mathcal{H}[\mathcal{K}_3(x;\gamma)]$ . The remaining eigenvalues of this operator must be identified by using numerical analysis. Note that the spectral problem now depends on two parameters: the coupling constant  $\Omega$  and the family parameter  $\gamma$ . In all investigated cases, the existence of a unique negative eigenvalue has been verified. Figure 6 shows the eigenvalues of the  $\mathcal{H}[\mathcal{K}_3(x;\gamma)]$  operator as a function of the family parameter  $\gamma$  for the values  $\Omega = 0.3$  and  $\Omega = 0.8$ .

The previous result is theoretically supported by applying Morse theory to the space of the orbits traced by the solutions. It can be verified that all the members of the  $\mathcal{K}_3(x;\gamma)$  family cross the point  $((-1)^\alpha \Omega, 0)$  [depending on the value of  $\alpha$  in (25)]. This implies the existence of a negative eigenvalue in the spectrum of the operator  $\mathcal{H}[\mathcal{K}_3(x;\gamma)]$ . In this scenario, the hypotheses of Theorem 3 in [16] are recovered and the claim stated there is now valid. Because these solutions verify that  $\frac{dQ[\mathcal{K}_3(x;\gamma)]}{d\omega} > 0$ , this means that the solutions in the  $\mathcal{K}_3(x;\gamma)$  family are unstable.

We complete this stability analysis by noting that the  $\mathcal{K}_2(x)$  solutions involve absolute stability. Again, the topological nature of the kink in the real component provides these defects with this property. A heuristic argument proving this fact is as follows. The energy of plane wave solutions around the vacua  $v_\pm$  in the complex component with Noether charge  $Q$  is given by  $E_{\text{free}} \approx \sigma Q$ ,

see [2,19]. However, the topological kink in the real component cannot decay into one of the vacua. Indeed, the fact that plane waves are defined in the complex component implies that the topological kink found in this configuration must correspond to that of the  $\mathcal{K}_1(x)$  solution (19). Now, we have to compare the energy of the  $\mathcal{K}_2(x)$  defect with that of this vibrating  $\mathcal{K}_1(x)$  solution. It can be checked that

$$E[\mathcal{K}_2(x, t)] < E[\mathcal{K}_1(x, t)] + \sigma Q[\mathcal{K}_2(x)],$$

which confirms that the  $\mathcal{K}_2(x, t)$  defects are stable with respect to decay into free particles.

#### IV. SUMMARY

In this paper, the existence of defects involving the coupling between kinks and  $Q$ -balls has been investigated in a one-parameter family of field theories in  $(1+1)$  dimensions with a real and a complex field. It has been found that there exist three types of solutions:  $\mathcal{K}_1(x)$  solutions (formed by only one topological kink),  $\mathcal{K}_2(x)$  solutions (which consist of a topological kink together with a  $Q$ -ball), and the one-parameter family of  $\mathcal{K}_3(x;\gamma)$  solutions (where a  $Q$ -ball is combined with a nontopological soliton). All of these solutions have been analytically identified. In addition, the second of the previously mentioned solutions can be considered as a counterexample of the universality of the Theorem 3 introduced in the seminal paper [16]. The small fluctuation operator evaluated on the  $\mathcal{K}_2(x)$  solutions has no negative eigenvalues and the derivative of the Noether charge of these defects with respect to the frequency is positive. However, the  $\mathcal{K}_2(x)$  solutions are stable. The topological charge of the kink living in the real component seems to prevent the  $Q$ -ball from decaying into the vacuum. From this point of view, these solutions involve novel properties with respect to the usual  $Q$ -balls arising in the literature. Finally, the family of  $\mathcal{K}_3(x;\gamma)$  defects are unstable. In this case, the previously mentioned theorem can be applied to prove this behavior.

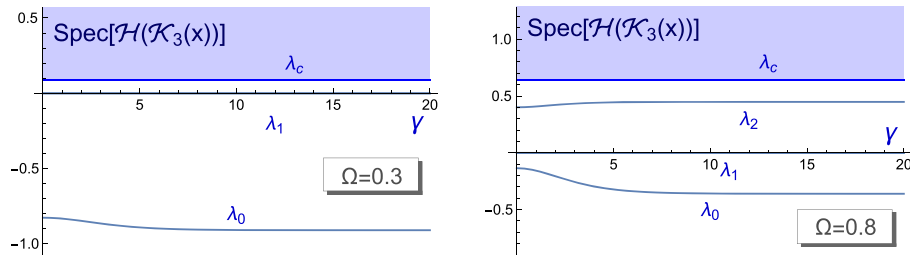


FIG. 6. Spectrum of the second-order small fluctuation operator  $\mathcal{H}[\mathcal{K}_3(x)]$  as a function of the family parameter  $\gamma$  for the values of the coupling constant  $\Omega = 0.3$  and  $\Omega = 0.8$ .

## ACKNOWLEDGMENTS

This research was funded by the Spanish Ministerio de Ciencia e Innovación (MCIN) with funding from the European Union NextGenerationEU (PRTRC17.I1) and

the Consejería de Educación, Junta de Castilla y León, through QCAYLE project, as well as MCIN Project No. PID2020-113406GB-I00 MTM.

- 
- [1] Y. M. Shnir, *Topological and Non-Topological Solitons in Scalar Field Theories* (Cambridge University Press, Cambridge, England, 2018).
- [2] T. D. Lee and Y. Pang, *Phys. Rep.* **221**, 251 (1992).
- [3] A. Kusenko and M. Shaposhnikov, *Phys. Lett. B* **418**, 46 (1998).
- [4] K. Enqvist and A. Mazumdar, *Phys. Rep.* **380**, 99 (2003).
- [5] M. Fujii and K. Hamaguchi, *Phys. Rev. D* **66**, 083501 (2002).
- [6] M. Fujii and K. Hamaguchi, *Phys. Lett. B* **525**, 143 (2002).
- [7] S. Kasuya and M. Kawasaki, *Phys. Rev. D* **64**, 123515 (2001).
- [8] J. McDonald, *J. High Energy Phys.* 03 (2001) 022.
- [9] M. Dine and A. Kusenko, *Rev. Mod. Phys.* **76**, 1 (2003).
- [10] S. I. Mukhin, *Condens. Matter* **7**, 31 (2022).
- [11] S. I. Mukhin, *Ann. Phys. (Amsterdam)* **447**, 169000 (2022).
- [12] S. I. Mukhin, *Condens. Matter* **8**, 16 (2023).
- [13] G. Campi, L. Barba, N. D. Zhigadlo, A. A. Ivanov, A. P. Menushenkov, and A. Bianconi, *Condens. Matter* **8**, 15 (2023).
- [14] Yu. M. Bunkov and G. E. Volovik, *Phys. Rev. Lett.* **98**, 265302 (2007).
- [15] S. Autti, P. J. Heikkinen, G. E. Volovik, V. V. Zavjalov, and V. B. Eltsov, *Phys. Rev. B* **97**, 014518 (2018).
- [16] R. Friedberg, T. D. Lee, and A. Sirlin, *Phys. Rev. D* **13**, 2739 (1976).
- [17] N. G. Vakhitov and A. A. Kolokolov, *Radiophys. Quantum Electron.* **16**, 783 (1973).
- [18] A. A. Kolokolov, *J. Appl. Mech. Tech. Phys.* **14**, 426 (1973).
- [19] M. I. Tsumagari, E. J. Copeland, and P. M. Saffin, *Phys. Rev. D* **78**, 065021 (2008).
- [20] S. Coleman, *Nucl. Phys.* **B262**, 263 (1985).
- [21] S. Coleman, *Nucl. Phys.* **B269**, 744 (1986).
- [22] A. Kusenko, *Phys. Lett. B* **404**, 285 (1997).
- [23] E. Y. Nugaev and M. N. Smolyakov, *J. High Energy Phys.* 07 (2014) 009.
- [24] A. Alonso-Izquierdo and C. Garzón Sánchez, *Physica D (Amsterdam)* **449**, 133764 (2023).
- [25] K. M. Lee, J. A. Stein-Schabes, R. Watkins, and L. M. Widrow, *Phys. Rev. D* **39**, 1665 (1989).
- [26] K. N. Anagnostopoulos, M. Axenides, E. G. Floratos, and N. Tetradis, *Phys. Rev. D* **64**, 125006 (2001).
- [27] X. Z. Li, J. G. Hao, D. J. Liu, and G. Chen, *J. Phys. A* **34**, 1459 (2001).
- [28] A. G. Panin and M. N. Smolyakov, *Eur. Phys. J. C* **79**, 150 (2019).
- [29] R. Jackiw and E. J. Weinberg, *Phys. Rev. Lett.* **64**, 2234 (1990).
- [30] J. Hong, Y. Kim, and P. Y. Pac, *Phys. Rev. Lett.* **64**, 2230 (1990).
- [31] M. Deshaies-Jacques and R. MacKenzie, *Phys. Rev. D* **74**, 025006 (2006).
- [32] A. M. Safian, R. Coleman, and M. Axenides, *Nucl. Phys.* **B297**, 498 (1988).
- [33] A. M. Safian, *Nucl. Phys.* **B304**, 392 (1988).
- [34] M. Axenides, E. Floratos, and A. Kehagias, *Phys. Lett. B* **444**, 190 (1998).
- [35] D. Bazeia, M. A. Marques, and R. Menezes, *Eur. Phys. J. C* **76**, 241 (2016).
- [36] D. Bazeia, L. Losano, M. A. Marques, R. Menezes, and R. Da Roucha, *Phys. Lett. B* **758**, 146 (2016).
- [37] R. B. MacKenzie and M. B. Paranjape, *J. High Energy Phys.* 08 (2001) 003.
- [38] A. Alonso-Izquierdo, *Phys. Scr.* **94**, 085302 (2019).
- [39] C. Montonen, *Nucl. Phys.* **B112**, 349 (1976).